Journal of Heat and Mass Transfer Research

Journal homepage: http://jhmtr.journals.semnan.ac.ir

Semnan University

# Numerical Study of Spherical Vapor Layer Growth Due to Contact of a Hot Object and Water

**Ali Jahangiri***

*Faculty of Mechanical & Energy Engineering, Shahid Beheshti University, Tehran, Iran*

**PAPER INFO**

***Paper history:***
Received: 2017-10-19
Received: 2018-02-11
Accepted: 2018-02-16

***Keywords:***
Hot body;
Vapor layer;
Vapor explosion;
Heat transfer;
Interface surface.

**ABSTRACT**

Vapor film formation and growth due to contact of a hot body and other liquids arise in some industrial applications including nuclear fuel rods, foundry and production of paper. The possibility of a steam explosion remains in most of these cases which could result in injuries and financial damage. Due to the importance of such phenomenon, this study deals with vapor layer forming, growth, and its internal pressure. A mathematical model of a molten spherical droplet immersed in water has been developed, and the results of the numerical solution are discussed. The effects of changing various characteristics (e.g. hot body size, temperature, and hydrostatic effects, as well as the temperature of bulk fluid) were investigated. These parameters affect the vapor layer size, vapor internal pressure, and the saturated temperature at the interface between vapor and liquid phases. Finally, conclusions indicate that the internal vapor pressure jumps, being up to several times larger than that of the initial condition. These pressure pulses and related vapor layer thickness variations could cause thermal fragmentation of the droplet which in turn results in strong pressure shock build-up due to small pieces of the droplet in contact with the water, which could then escalate to become a propagating large-scale vapor explosion. The vapor explosions could be hazardous and threaten the system safety.

DOI: 10.22075/jhmtr.2018.12775.1192



## 1. Introduction

It is important to study the heat transfer process in bubbles or vapor layers formed at the surfaces of hot objects immersed in liquids sincethis phenomenon might occur in the nuclear energy industry, metal melting, glazing, and also when magma falls into the sea [1, 2]. Sometimes, vapor layer growth may bring a catastrophe. As an instance, melted nuclear fuel rod pieces can fall into the reactor coolant that may cause the vapor explosion to occur like what happened in Ukraine's Chernobyl power plant in 1986 [3].

The vapor explosion phenomenon arises from the extreme heat exchange between a hot body (a droplet of warmish metal) contact with a relatively volatile material (e.g. water), wherein the molten metal undergoes fine fragmentation. Consequences of extreme heat exchange and Rapid Phase Transition (RPT), vapor film pressure around a finely fragmented hot body enlarges sharply in a short time and can result in a vapor layer internal shock wave which weakens the coolant casing [1]. There are beneficial utilizations of vapor film explosions. For example, at an ink-jet printer, small vapor bubble explosions are used to carry the ink out of the cartridge [4]. The acoustical lithotripsy for kidney stones and laser surgical operations is another file which forms and explodes vapor bubbles [1].

Some of the important relevant research works are summarized as follow.

As the pioneers in vapor explosions field, Nelson and Duda [5], surveyed vapor layer formation and initiation of a vapor explosion when molten iron oxide immersed in water. They found that the permeation of non-condensable gases into the vapor layer formed around the molten drop prevented the onset of spontaneously vapor explosion.

*Corresponding Author: A. Jahangiri, Faculty of Mechanical and Energy Engineering, Shahid Beheshti University, Tehran, Iran.
Email: a_jahangiri@sbu.ac.ir

They also showed that a specified characteristic of the system (including the molten drop and its film) is its symmetry because this process occures at entire drop area.

Cao et al. [6] studied the interplay between the molten materials and cooling fluid. They also considered the effect of a sudden pressure change applied on the system from the external environment on the mechanism of fragmentation during a vapor film explosion. They showed that, after vapor film destruction and contact between cooling fluid and molten material surface, a pressure wave was formed at the surface of the molten material. This resulted in formation of a new bubble, rapidly growing on the molten surface, with this recently formed bubble also collapsing. Finally, their results were compared with experimental observations of Ciccarelli and Frost [7], and it was found that the vapor layer growth on the surface of molten material obtained in the calculation was similar to the results obtained from their experiments.

By experimental study on the situation that can occur in a nuclear reactor, Abe et al. [8 , 9] assessed the triggering part of vapor explosion. Employing a high speed camera which produces 40500 digital frames/second to capture images of the contact between cooling fluid and molten material surface, transient vapor layer collapsed and changes in its pressure were recorded.

In another research by Gubaidullin and Sannikov [10], the kinetic treatment and transport phenomena of vapor films created on the surface of hot copper spheres was investigated numerically. Applying two numerical simulations in spherical coordinate and considering that vapor thermal conductivity varies linearly, they obtained dimensionless vapor layer radius versus time. They proved that the dependency of blobs radius to the radius ratio of particles with no dimension does not differ for all blobs having a different level of radii.

In addition to the previous research, others have also referred to this phenomenon [11-16]. The time-dependent process for a Warmish object plunged vaporizable liquids has not been fully surveyed taking into account non-equilibrium conditions and temperature changes at the vapor-liquid phase interface. It is difficult hence to study different thermophysical phenomena. For the complete investigation, it is necessary to provide an appropriate model which offers details of heat transfer in the various phases. The present study has focused on vapor layer size and its internal pressure change which can be used to point the system safety.

## 2. Modeling and Methodology

For the present study, a hot copper sphere is assumed to be immersed at a specific depth within water. A thin vapor film exists on the hot copper surface at the beginning of the process. To investigate the vapor film growth as a function of time, it is necessary to consider the governing equations including the continuity, the momentum and energy conservation for the liquid, presented in general form in Eqs. (1) to (3), respectively [17].

$$\frac{D\rho_l}{Dt} + \rho_l \vec{\nabla}.\vec{u} = 0 \tag{1}$$

$$\rho_l \frac{D\vec{u}}{Dt} = -\nabla P + \mu \nabla^2 \vec{u} + \vec{\mathrm{F}} \tag{2}$$

$$\rho_l C_l \frac{DT}{Dt} = \vec{\nabla}.\left(k\vec{\nabla}T\right) + q''' + \mu\emptyset \tag{3}$$

Initial sphere and water temperatures, pressure and temperature at the free surface of the water, and depth of the sphere center below the water free surface are assumed to be known. Surface tension is included with a viscous term at the vapor-liquid interface and the occurrence of heat transfer through the vapor layer is intended by conduction only.

The vapor layer is assumed to be spherical for the entire process. If the heat flux emitted by the hot copper surface is large enough for boiling [14, 18], the vapor layer growth maintains. Otherwise, the vapor condenses and the vapor layer would fail.

Due to the one-dimensional geometry and the spherical symmetry of the phenomenon, Eq. (1) could be simplified into:

$$\frac{d}{dr}(r^2 u) = 0 \tag{4}$$

It is assumed that the outside spherical shape of the vapor film is maintained during the process modelled herein. Eq. (2) is the momentum in spherical coordinates, wherein body forces and viscous terms are negligible, and can be considered as:

$$\frac{\partial u}{\partial t} + u\frac{\partial u}{\partial r} = -\frac{1}{\rho_l}\frac{\partial P}{\partial r} \tag{5}$$

Vapor-liquid phase boundary speed is computed with the help of conservation of mass at the vapor-liquid interface as:

$$\frac{dm_v}{dt} = -\frac{dm_l}{dt} \; or \; \rho_v A u_v = -\rho_l A u_l \tag{5a}$$

Considering related velocity between liquid and vapor at the vapor-liquid interface and solution of Eq. (5a), the inward velocity of liquid relative to the interface is given by $-\frac{\rho_v}{\rho_l}\frac{dR_v}{dt}$, thus:

$$u(R_v,t) = \frac{dR_v}{dt} + u_l = \frac{dR_v}{dt} - \frac{\rho_v}{\rho_l}\frac{dR_v}{dt} = \left(1 - \frac{\rho_v}{\rho_l}\right)\frac{dR_v}{dt} \tag{6}$$

Integrating Eq. (4) from 'Rv' to r, and considering the vapor-liquid interface condition (Eq. (5a)) gives:

$$u(r,t) = u(R_v,t)\left(\frac{R^2}{r^2}\right) \tag{7}$$

Then inserting Eqs. (6) and (7) into Eq. (5) yields [19]:

$$\frac{1}{r^2}\left(1 - \frac{\rho_v}{\rho_l}\right)\frac{d}{dt}\left(R_v^2\dot{R}_v\right) - \frac{2}{r^5}\left(1 - \frac{\rho_v}{\rho_l}\right)^2 R_v^4\dot{R}_v^2 = -\frac{1}{\rho_l}\frac{\partial P}{\partial r} \tag{8}$$

where, $\dot{R}_v = \frac{dR_v}{dt}$ is vapor film boundary changes with time but not absolute total velocity (the rate of movement of the interface). $u_l = -\frac{\rho_v}{\rho_l}\frac{dR_v}{dt}$ is relative velocity (the inward velocity of liquid relative to the interface (phase transition rate)). $u(R_v, t)$ is the absolute velocity of vapor film. $u(r, t)$ is velocity profile for radial direction. Eq. (8) should be integrated from 'Rv' to ∞. For pressure boundary conditions, the hydrostatic pressure equation ($P_\infty = P_b + \rho_l gh$) should be applied at the free surface and the pressure difference between vapor and liquid phases at the vapor-liquid interface should be used, which is obtained by Laplace's equation and viscous shear stress at the vapor-liquid interface as [20]:

$$P_v - P_l = -2\mu \left|\frac{\partial u}{\partial r}\right|_{r=R_v} + \frac{2\sigma}{R_v} \quad (9)$$

The final vapor film growth equation becomes then:

$$\left(1-\frac{\rho_v}{\rho_l}\right)\left[R_v\ddot{R}_v + 2\dot{R}_v^2 + 4\frac{\mu}{\rho_l}\frac{\dot{R}_v}{R_v} - \left(1-\frac{\rho_v}{\rho_l}\right)\frac{\dot{R}_v^2}{2}\right] = -\frac{1}{\rho_l}\left[P_b + \rho_l gh - P_v + \frac{2\sigma}{R_v}\right] \quad (10)$$

$$\dot{R}_v(t=0) = 0 \;\&\; R_v(t=0) = R_w + \delta(1)$$

where, $\ddot{R}_v = \frac{d^2R_v}{dt^2}$ is acceleration at the vapor-liquid surface and since it is assumed that a thin vapor film exists on the sphere surface initially, δ(1) is assumed initial vapor film thickness. If tension of surface, viscosity and $\frac{\rho_v}{\rho_l}$ are removed from recent equation, the familiar Rayleigh equation will be given [20]. The vapor-liquid interface temperature is usually considered to be the saturated temperature (Tsat). Its pressure and the temperature at saturated conditions are related by the Clausius-Clapeyron equation, where water vapor is assumed to be a perfect gas [21].

$$\frac{dP_v}{dT_{sat}} = \frac{h_{fg}}{\left(\frac{1}{\rho_v}-\frac{1}{\rho_l}\right)T_{sat}}, P_v = \rho_v R_{H_2O} T_{sat} \quad (11)$$

## 3. Heat exchange through the vapor layer

When the layer of vapor has small internal mass, changes in its energy is negligible. Therefore, the flux of heat induced by the hot surface will be transmitted entirely to the vapor-liquid juncture. Fig. 1, illustrates the part of this transferred heat flux leads water to evaporate and the remaining flux is transmitted to the liquid phase.

Commonly, the transfer of heat through the vapor layer, occurs simultaneously by thermal conduction and advection. Regarding the equivalent thermal conductivity (keq) which is used generally, the heat transfer is calculated as:

$$Q_i = Q_w \Rightarrow Q_i = q_i''(4\pi R_v^2) = q_w''(4\pi R_w^2) = Q_w \quad (12)$$

Given that values are calculated at average temperature and Gr×Pr<103, with a good approximation, keq can be considered as vapor thermal conductivity ($k_v$) [22]. The heat flux emitted by the hot copper surface equals

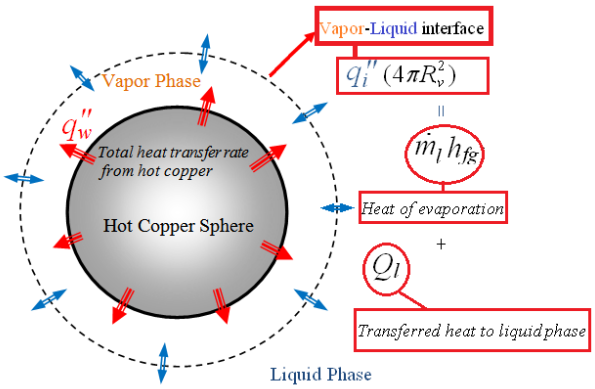


**Figure 1.** General geometry of problem and energy transfer at boundaries

$$q_w'' = k_v \frac{T_w(t) - T_{sat}(t)}{R_v(t) - R_w}\frac{R_v(t)}{R_w} + q_{rad}'' \quad (13)$$

Due to the spherical geometry of the phenomena, the copper surface heat flux and the heat flux through the vapor-liquid interface can be related as:

$$q_i'' = q_w''\left(\frac{R_w}{R_v(t)}\right)^2 \quad (14)$$

By combining the Eqs. (13) and (14), the heat flux through the vapor-liquid interface would be calculated as:

$$q_i'' = k_v \frac{T_w(t) - T_{sat}(t)}{R_v(t) - R_w}\frac{R_w}{R_v(t)} + q_{rad}''\left(\frac{R_w}{R_v(t)}\right)^2 \quad (15)$$

Since during this process, the temperature of the vapor layer and accordingly its thermal conductivity is not constant, the average temperature of the Tw (t) and Tsat (t) is used to specify thermophysical properties.

In addition, due to the high copper surface temperature, the radiation heat transfer cannot be ignored ($\frac{q_{rad}''}{q_i''(t=0)} \approx 0.2$) and related radiation heat flux is calculated as:

$$q_{rad}'' = \varepsilon\sigma(T_w^4(t) - T_{sat}^4(t)) \quad (16)$$

Wherein ε≈0.15 and view factor =1 [23].

Since the vapor layer growth progresses rapidly, the hot copper sphere's temperature is calculated using the lumped capacity method, written as [14, 23].

$$q_w'' A_w = -m_w C_w \frac{dT_w}{dt} \quad (17)$$

$$q_w''(4\pi R_w^2) = -\rho_w\left(\frac{4}{3}\pi R_w^3\right)C_w\frac{dT_w}{dt} \Rightarrow \frac{dT_w}{dt} = -\frac{3q_w''}{\rho_w R_w C_w} \quad (18)$$

By substituting the copper surface heat flux (Eq. (13)) into Eq. (18), the following expression could be achieved:

$$\frac{dT_w}{dt} = -\frac{3k_v[T_w(t) - T_{sat}(t)]R_v(t)}{\rho_w R_w^2 C_w(R_v(t) - R_w)} \quad (19)$$

Differential Eq. (19) is solved by considering the initial condition ($T_w = 1356\,K\ at\ t = 0$) and using a numerical approach (Runge-Kutta) [24]. Then, the

sphere's surface cooling process which is varied with time would be obtained.

An appropriate connective heat transfer coefficient $\bar{h}$, requires determining energy transferred to liquid phase evaporation and energy balance (Fig. 1). The heat transfer rate can be rewritten as follows [25].

$$\begin{aligned} & q_l''(4\pi R_v^2) = Q_i - \dot{m}_l h_{fg} \\ & q_l'' = \bar{h}(T_{sat} - T_\infty) \\ & \bar{h}(T_{sat} - T_\infty)(4\pi R_v^2) \\ & = k_v \frac{T_w(t) - T_{sat}(t)}{R_v(t) - R_w} \frac{R_w}{R_v(t)} (4\pi R_v^2) - \dot{m}_l h_{fg} \end{aligned} \quad (20)$$

$$\begin{aligned} & \bar{h}(W/m^2K)) = 1.95\left(q_l''(W/m^2)\right)^{0.72}\left(P\ (bar)\right)^{0.24} \\ & 10^4(W/m^2) \le q_l'' \le 10^6(W/m^2) \\ & 0.5(bar) \le P \le 20(bar) \end{aligned} \quad (21)$$

Finally, it should be noted that density of vapor phase [26] and latent heat of evaporation [27-30] at the interface are strongly affected by saturations condition. Eqs (22) and (23) are used to consider the variation of vaporization latent heat and vapor layer density as function of saturation conditions, respectively. The constants used in these equations are provided in the references [26, 27].

$$\begin{aligned} & h_{fg} = h'_{fg}\left[\frac{1 - T_r}{1 - T'_r}\right]^{0.38} \\ & T_r = \frac{T_{sat}}{T_{crit}} \\ & h'_{fg}\ \&\ T'_r\ are\ considered\ at\ 100^oC\ and\ 101.3\ kPa \end{aligned} \quad (22)$$

$$\begin{aligned} & Ln\left(\frac{\rho_v}{\rho_{crit}}\right) = c_1(1 - T_r)^{2/6} + c_2(1 - T_r)^{4/6} \\ & + c_3(1 - T_r)^{8/6} + c_4(1 - T_r)^{18/6} + c_5(1 - T_r)^{37/6} \\ & + c_6(1 - T_r)^{71/6} \end{aligned} \quad (23)$$

## 4. Validation

A computer algorithm was provided to calculate Eqs. (10), (19) and (20) simultaneously. For time step convergence analysis, the time steps were selected to be small enough to minimize the effects on obtained results at 10-6 range of errors.

Also, results were compared with numerical work of Gubaidulin and Sanikov [10] in which modeled interaction between a hot (1356 K) copper sphere and liquid water at 368 K. They obtained dimensionless radius ($R_v^* = \frac{R_v}{R_w}$) variation of the vapor film versus dimensionless time ($t^* = \frac{t}{t_l}$) using two methods. In which, $t_l$ is the characteristic time (0.238 s) of heat propagation in the liquid phase.

Fig. 2 has ensured the agreement of vapor layer size trends. Disagreement of numerical values in Fig. 2, results in ignorance of radiation heat flux, $h_{fg}$ and $\rho_v$ by Gubaidulin and Sanikov at model No. 1 and also in addition to vapor bubble oscillation in the model No. 2.

## 5. Results and discussion

Variation of hot body size, temperature, and hydrostatic effects, temperature of bulk fluid and vapor film initial thickness may lead to different results which are discussed in this section.

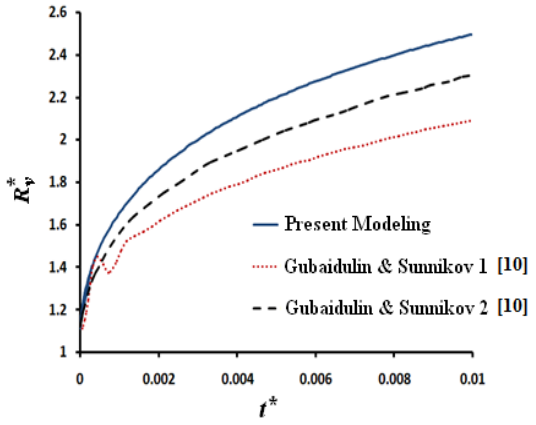


**Figure 2.** Comparison between results for dimensionless vapor film radius versus dimensionless time using 3 different methods

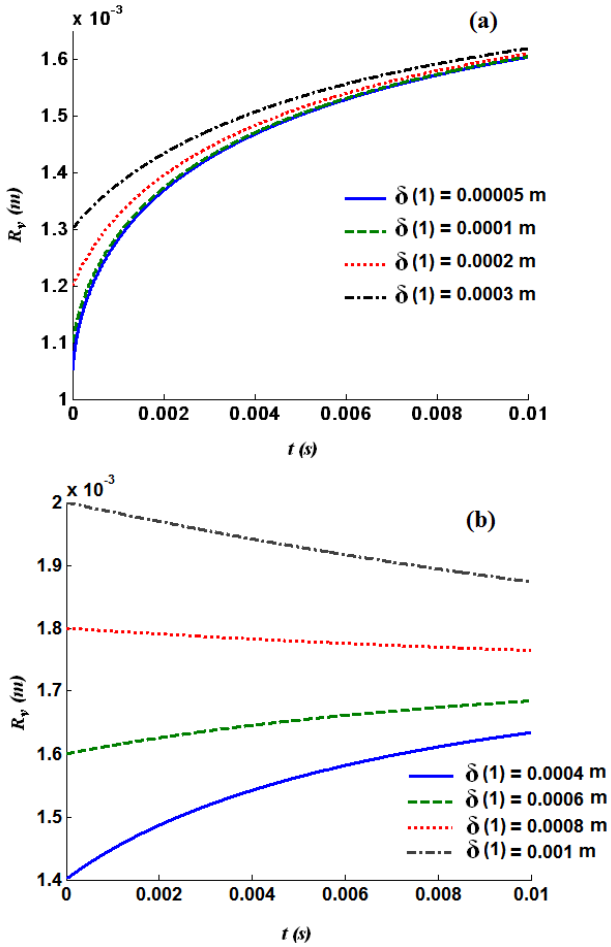


**Figure 3.** Vapor film radius change versus time based on assumed initial thicknesses of the vapor film, (a): δ(1) is less than 0.0003 m, (b): δ(1) is more than 0.0004 m

Temperature change versus time for sphere is modeled using lumped capacity method. This model shows in the first 0.01 s, the sphere's surface temperature decreases negligibly for variation of hot body size, temperature, and hydrostatic effects, water temperature and the vapor layer initial thickness.

### 5.1. The change of the vapor layer initial thickness

The fact that mathematical model is not suitable for describing the process onset (when a hot particle fallen into water is not encircled with the vapor film yet), must assign the initial conditions arbitrarily. Therefore, current calculations assumed that a thin vapor film exists on the sphere surface initially which is indicated by δ(1). In this section, the effect of the initial vapor film thickness variation is considered for the case of contact between the sphere (1 mm radius at 1356 K) and water at 368 K when the sphere is 1 cm below the water surface.

As shown in Fig. 3(a) and 3(b), higher vapor film initial thickness excessing the specified maximum brings the vapor layer reduction rather than growth. Indeed, the growing of the layer considering the mathematical simulation of this phenomenon has a maximum amount about i.e. initial thickness (1.7 mm - 1 mm = 0.7 mm). When initial thickness (δ(1)) is more than 0.7 mm, the vapor layer size will be reduced.

As shown in Fig. 4(a) and 4(b), the vapor layer maximum internal pressure and liquid-vapor interface saturated temperature decrease corresponding to an increase in vapor layer initial thickness.

The main reason of decrease in the maximum internal pressure and the saturated temperature is reduction of the energy needed for the vapor layer growth to its maximum amount due to the assumed higher vapor layer initial thickness (in fact, vapor layer grows to maximum amount with lower heat transfer).

In order to investigate the effects of the other parameters, a reasonable initial thickness of vapor layer should be chosen in all following analyses. Hence, for estimating the initial vapor layer thickness, Eq. (24) is considered at the beginning of the process [18]. $t_l$= 1e-6 s was assumed at the onset of this process. Then, the calculated radius is 4.5e-4 m from Eq. (24). Considering this computed radius makes it reasonable to choose initial vapor film radius as 0.0001 m [18].

$$for\ \ t^+ = t\frac{A^2}{B^2} \ll 1 \Rightarrow R_v(t) \approx At$$

$$A = \left[b\frac{\rho_v h_{fg}\Delta T_{sat}}{\rho_l T_{sat}}\right]^{0.5}, \qquad \Delta T_{sat} = (T_w - T_{sat})$$

$$b = \frac{\pi}{7}, B = \left[\frac{12}{\pi}Ja^2\alpha_l\right]^{0.5}, \qquad \alpha_l = \left[\frac{k_l}{\rho_l C_l}\right]$$

$$Ja = \frac{\rho_l C_l \Delta T_{sat}}{\rho_v h_{fg}}$$

### 5.2. The variations of the copper hot sphere size

The effect of the sphere radius variation is investigated for the case of contact between the sphere at 1356 K and water at 368 K, for the sphere being 1 cm below the liquid surface.

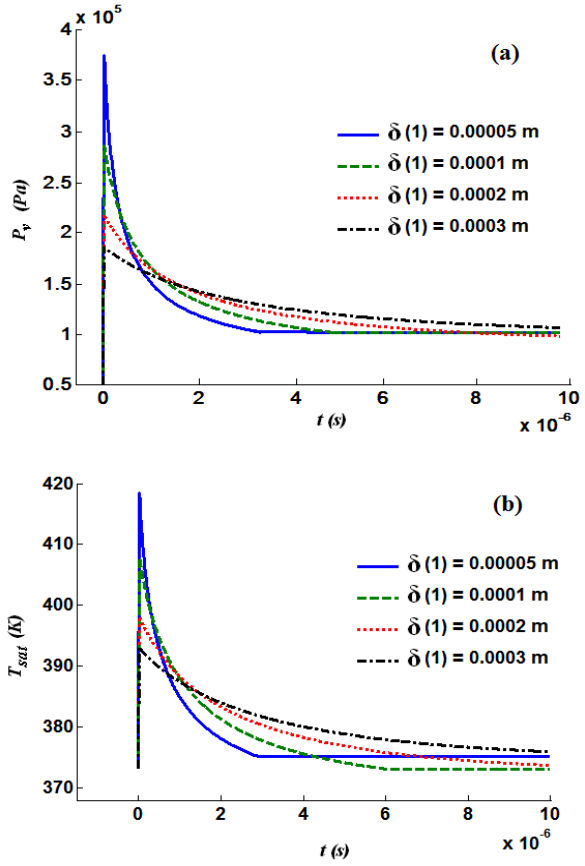


**Figure 4. (a):** Saturation temperature on phase interface, (b): Vapor film pressure change versus time based on assumed initial thicknesses of the vapor film

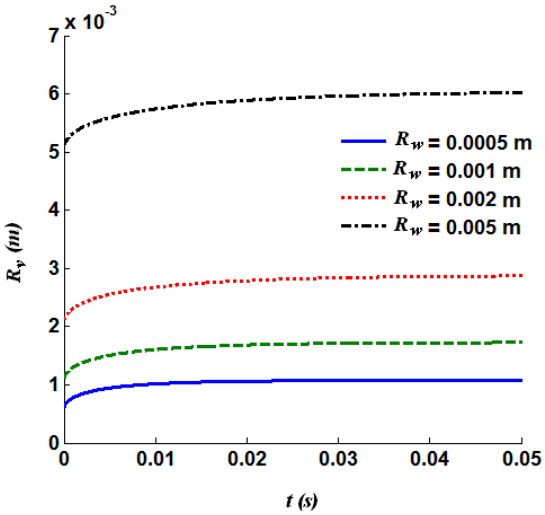


**Figure 5.** Vapor film radius change versus time based on various sphere radiuses.

As mentioned previously in Section 2.1, for using the kv instead of keq in Eq. (12), the condition Gr×Pr $< 10^3$ should be satisfied. The variation radius is limited up to 5mm because the Grashof number will not be satisfied for radii greater than 5mm.

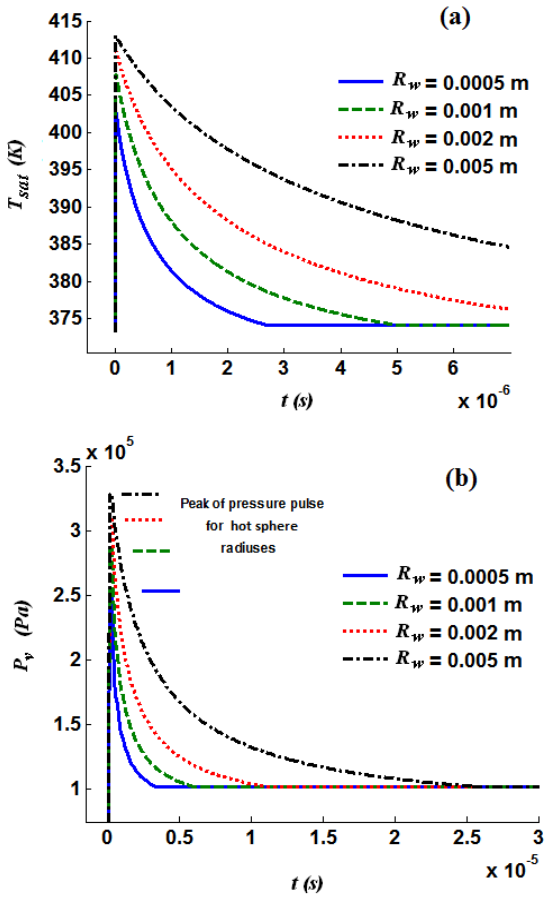


**Figure 6. (a):** Saturation temperature on phase interface, (b): Vapor film pressure change versus time based on various sphere radiuses

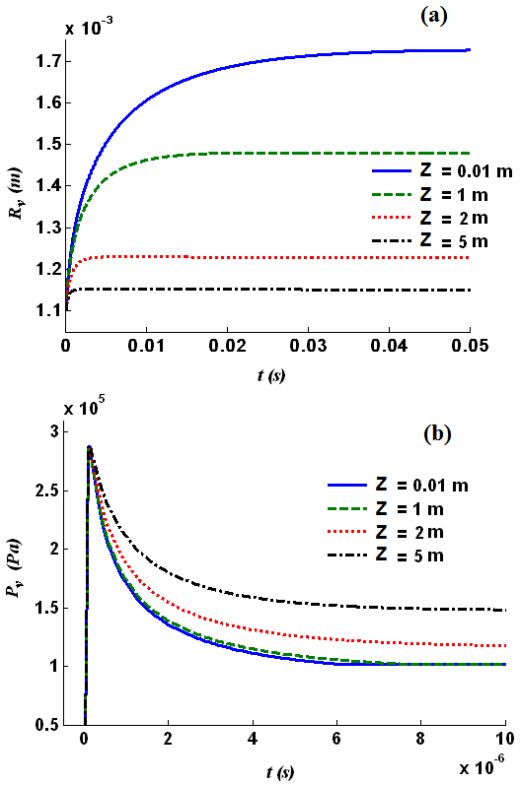


**Figure 7.** Vapor film changes versus time based on various depths of the sphere's center below the water's free surface (a): Vapor film radius change, (b): Pressure inside vapor film change

As shown in Fig. 5, the expected film thickness growth is more in higher sphere temperatures which is because of heat generated-flux effect on copper surface. However, in Figs. 6(a) and 6(b), it can be seen that as the hot copper sphere radius increases, the heat generated-flux on copper surface increases. It is expected that the corresponding saturated temperature as well as the maximum internal pressure jump of the vapor layer increase.

### 5.3. The hydrostatic effects

In this section, the hydrostatic effects which changing the depth of the sphere center inside water are investigated for the case of contact between the sphere (1 mm radius at 1356 K) and water at 368 K.

The vapor film thickness is inversely proportional to the increased depth of the sphere in water because of the hydrostatic pressure increase as shown in Fig. 7(a), which results in slower vapor layer growth. As Fig. 7(b)) depicts, the maximum pressure jump of the vapor layer remains constant, owing to the non-variance in the phase contact surface heat flux with the depth increase of sphere water placement.

### 5.4. Initial temperature of hot body

This section demonstrates the effect of initial temperature changes of sphere for the case of contact between the sphere (1 mm radius) with water at 368 K when the sphere is 1 cm below the water surface.

In order to provoke the vapor layer growth, the initial heat flux should be higher than the critical amount. At lower temperatures, the vapor film thickness is more likely to decrease. Fig. 8(a) shows that for the surface temperature lower than 730 K, not only lessens the possibility of increase in the vapor film growth but also causes collapsed. The low temperatures results in formation of insufficient heat transferred on the surface of the sphere that is not be sufficient to support the vapor film and its growth. As illustrated in Fig. 8(b), the heat flux that reaches the phase interface increases with the increasing initial temperature of the sphere. This results in increased quantity of the internal vapor layer maximum pressure.

### 5.5. Bulk water temperature changes

In this section, the effect of bulk water temperature changes is investigated for the case of contact between the sphere (1 mm radius at 1356 K) and water at 368 K when the sphere is 1 cm below the water surface.

A significant point in Fig. 9(a) and 9(b) is the effect of reducing the temperature of bulk water in the vapor film

thickness. Accordingly, in less than 340 K change of vapor film radius with lower initial vapor film thickness (based on Eq. (24)) at times below 0.0001 seconds is increased slightly. However, because of less difference between saturation and bulk water temperatures, at higher bulk temperature (bulk water is closer to the saturation condition) vapor film grows rapidly.

At lower water temperatures, further heat flux is needed for evaporation as illustrated in Fig. 10. It can be seen in Fig. 10 that more heat flux is needed for evaporation in lower water temperature. Hence, when the vapor layer grows and consequently heat flux reduces on phase interface surface, the corresponding saturation temperature and the maximum pressure pulse inside the vapor layer would decrease.

## 6. Conclusions

The aim of the present study was evaluation of the vapor layer generation, and growth due to contact between a hot spherical body and bulk water. The vapor layer initial thickness, hot body size, initial temperature, bulk water temperature, hydrostatic effects, the saturated temperature at the interface surface and the internal vapor layer pressure change, are the most effective parameters investigated in this article.

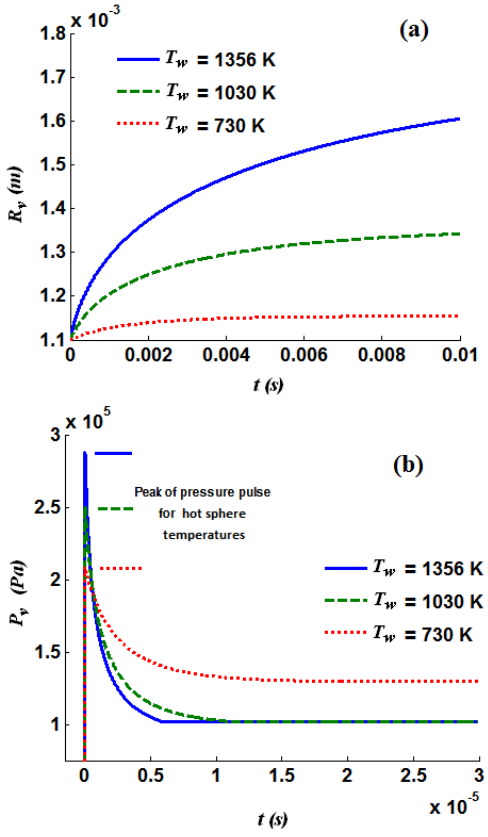


**Figure 8.** Vapor film changes versus time based on various initial temperatures of hot sphere (a): Vapor film radius change, (b): Pressure inside vapor film change.

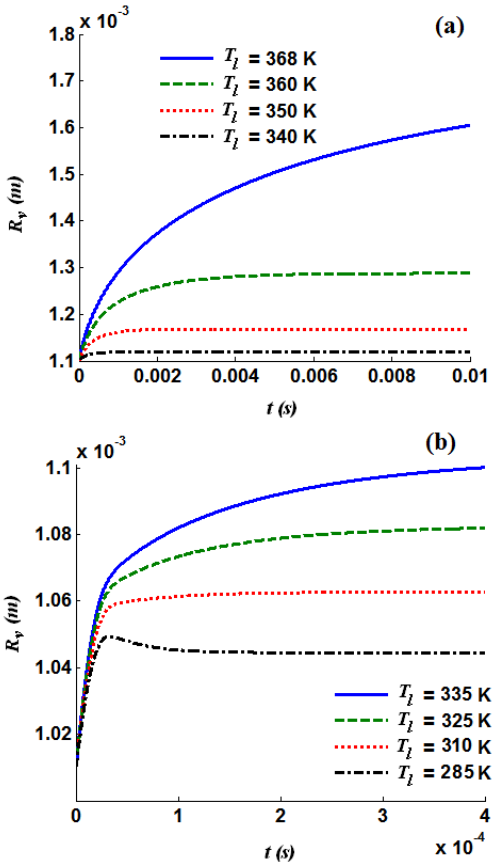


**Figure 9.** Vapor film radius change versus time based on various bulk water temperatures (a): bulk water temperatures more than 340 K, (b): bulk water temperatures less than 335 K

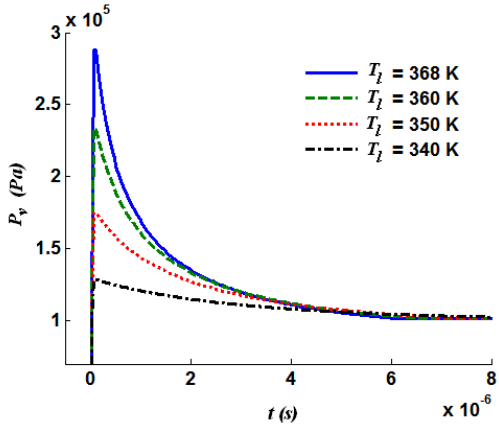


**Figure 10**. Pressure inside vapor film change versus time based on various bulk water temperatures

The numerical solutions for contact of water and hot spherical body, indicate the following results.

- If the calculated maximum vapor layer growth is less than the initial thickness, the thickness of the vapor layer will decrease. Also, it would also be confirmed that the vapor layer growth consistently converges to a certain amount.

- The hot sphere diameter growth could remarkably increase the thermal energy generation and water saturated temperature, so the maximum internal pressure of the vapor layer will be increased consequently.

The vapor layer thickness reduction is addressed as one of the most considerable effects of the hydrostatic pressure changes which itself is due to a change of the entrance depth of hot body into the water. Thus, because of the prevention of vapor layer growth, the total pressure on the outer interface of the spherical film would increase.

- The heat flux increased as a result of increasing the initial temperature of the hot body. It also increases the vapor layer thickness growth, its rate and vapor internal maximum pressure.
- Considering bulk water temperature change, it is obvious that bulk temperature reduction causes vapor layer growth as well as vapor layer maximum pressure to be reduced. These phenomena can be justified as requiring more thermal energy to overcome the temperature difference of bulk water and its corresponding saturated temperature.

Eventually, based on the assumed initial vapor layer thickness which is smaller than the equilibrium film thickness for given parameters, the maximum vapor layer pressure pulse can be abruptly increased even by 5 times. These pressure pulsations and related vapor layer thickness variations can cause the thermal fragmentation of a melt droplet, resulting in stronger pressure shock build-up due to the small fragments in contact with water, which could then escalate to become a propagating large-scale vapor explosion. The vapor explosions could be hazardous and may affect the system safety.

## Nomenclature

$A_w$ Hot sphere area ($m^2$)
A A parameter for calculating initial film thickness (m/s)
b A constant used in calculating initial film thickness (-)
B A parameter for calculating initial film thickness ($m/s^{0.5}$)
C Specific heat capacity (J/kg.K)
$C_l$ Specific heat capacity of liquid (J/kg.K)
$C_w$ Specific heat capacity of hot copper (J/kg.K)
g Gravitational acceleration (m/s2)
Gr Grashof number (-)
$\vec{F}$ Body force weight vector (N/m3)
h Depth of center of sphere in water (m)
$h_{fg}$ Evaporation latent heat (J/kg)
$h'_{fg}$ Evaporation latent heat at 100 oC & 1 bar(J/kg)
$\bar{h}$ Convection heat transfer coefficient ($W/m^2.K$)
Ja Jakob Number (-)
$k_{eq}$ Equivalent thermal conductivity (W/m.K)
$k_l$ Thermal conductivity of liquid water(W/m.K)
$k_v$ Thermal conductivity of vapor (W/m.K)
$m_l$ Mass of liquid phase (kg)
$m_v$ Mass of vapor phase (kg)
$m_w$ Mass of hot copper (kg)
$\dot{m}_l$ Mass flow rate of liquid phase (kg/s)
P Pressure (Pa)
$P_b$ Pressure at free surface of liquid (Pa)
$P_v$ Vapor pressure at vapor-liquid interface (Pa)
$P\infty$ Hydrostatic pressure (Pa)
Pr Prandtl number (-)
Qi Total heat transfer rate at vapor-liquid interface (W)
$Q_l$ Heat transferred to liquid phase (W)
$Q_w$ Total heat transfer rate from hot copper surface (W)
$q''_i$ Heat flux at vapor-liquid interface (W/m2)
$q''_l$ Transferred heat flux to liquid phase (W/m2)
$q''_{rad}$ Radiation heat flux (W/m2)
$q''_w$ Heat flux at hot sphere surface (W/m2)
$q'''$ Volumetric internal heat generation rate(W/m3)
r Spherical radial coordinate (m)
$R_{H_2O}$ Specific gas constant for water vapor (J/kg.K)
$R_v$ Vapor film radius (m)
$R_w$ Hot copper sphere radius (m)
$\dot{R}_v$ Vapor film boundary changes with time (m/s)
$\ddot{R}_v$ Vapor film acceleration in radial direction(m/s2)
$R^*_v$ Dimensionless vapor film radius (-)
t Time (s)
$t_l$ Characteristic time of thermal energy propagation (s)
t+ Dimensionless time for initial film thickness(-)
t* Dimensionless time (-)
T Temperature (K)
$T_{crit}$ Critical temperature of water (K)
$T_l$ Temperature of liquid water (K)
$T_r$ Reduced temperature (K)
$T_{sat}$ Saturation temperature (K)
$T_w$ Temperature of hot copper surface (K)
$T_\infty$ Temperature of liquid at free surface (K)
$\bar{T}$ Mean temperature (K)
$T'_r$ Reduced temperature at 100 oC & 1 bar (K)
u Velocity of the liquid (m/s)
ul Velocity of the liquid relative to vapor-liquid interface (m/s)
$u_v$ Velocity of the vapor relative to vapor-liquid interface (m/s)
$\vec{u}$ Velocity vector (m/s)
Z Depth of the sphere's center below the water's free surface (m)

**Greek symbols**

$\alpha_l$ Thermal diffusivity of liquid water (m2/s)

| | |
|---|---|
| $\delta$ | Vapor layer thickness (m) |
| $\delta(1)$ | Initial vapor layer thickness (m) |
| $\mu$ | Dynamic viscosity of liquid water (kg/m.s) |
| $\rho$ | Density (kg/m3) |
| $\rho_v$ | Density of vapor (kg/m3) |
| $\rho_l$ | Density of liquid (kg/m3) |
| $\rho_{crit}$ | Critical density of water at critical temperature (kg/m3) |
| $\sigma$ | Surface tension coefficient (kg/s2) |
| $\emptyset$ | Viscous dissipation term (1/s2) |

**Subscripts**

| | |
|---|---|
| crit | Critical state |
| eq | Equivalent |
| l | Liquid |
| rad | Radiate heat transfer |
| sat | Saturation |
| v | Vapor |
| w | Copper body wall |

## Acknowledgements

The financial support for this research, from the Shahid beheshti university G.C. (Grant No. 600/1025) is gratefully acknowledged.

## References

[1]Berthoud G. Vapor explosions, Annual Review of Fluid Mechanics. 32, 573-586, (2000).

[2]R. Thiery, L. Mercury, Explosive properties of water in volcanic and hydrothermal systems, Journal of Geophysical Research: Solid Earth, 114, (2009).

[3]M. Ragheb, Chernobyl accident", The history of Chernobyl nuclear power generation accident, Ukraine, (2010).

[4]K. Okuyama, S. Tsukahara, N. Morita, Y. Iida, Transient behavior of boiling bubbles generated on the small heater of a thermal ink jet printhead, Experimental Thermal and Fluid Science, 28, 25-834, (2004).

[5]L.S. Nelson, P.M. Duda, Steam explosion experiments with single drops of iron oxide melted with a CO2 laser, High Temperatures. High Pressures, 14, 259-281, (1982).

[6]X. Cao, R. Hajima, K. Furuta, S. Kondo, A numerical analysis of molten metal drop and coolant interaction, Journal of nuclear science and technology, 37, 1049-1055, (2000).

[7]G. Ciccarelli, D.L. Frost, Fragmentation mechanisms based on single drop steam explosion experiments using flash X-ray radiography, Nuclear engineering and design, 146, 109-132, (1994).

[8]Y. Abe, H. Nariai, Microscopic film collapse behavior at trigger for vapor explosion, HEAT TRANSFER, 3, 551-556, (2002).

[9]Y. Abe, H. Nariai, Y. Hamada, The trigger mechanism of vapor explosion, Journal of Nuclear Science and Technology, 39, 845-853, (2002).

[10]A.A. Gubaidullin, I. Sannikov, The dynamics and heat and mass transfer of a vapor bubble containing a hot particle, High temperature, 43, 922-929, (2005).

[11]V.V. Glazkov, V. Grigor'ev, V.G. Zhilin, Y.A . Zeigarnik, Y.P. Ivochkin, K.G.e. Kubrikov, N.y.V. Medvetskaya, A.A. Oksman, O.A.e. Sinkevich, A possible mechanism of triggering a vapor explosion, High temperature, 44, 908, (2006).

[12]K. Moriyama, S. Takagi, K. Muramatsu, H. Nakamura, Y. Maruyama, Evaluation of containment failure probability by ex-vessel steam explosion in Japanese LWR plants, Journal of nuclear science and technology, 43, 774-784, (2006).

[13]I. Dergunov, A. Kryukov, A. Gorbunov, The vapor film evolution at superfluid helium boiling in conditions of microgravity, Journal of Low Temperature Physics, 119, 403-411, (2000).

[14]N. Khabeev, O. Ganiev, Dynamics of a vapor shell around a heated particle in a liquid, Journal of applied mechanics and technical physics, 48, 525-533, (2007).

[15]A.P. Kryukov, A.K. Yastrebov, Analysis of the transfer processes in a vapor film during the interaction of a highly heated body with a cold liquid, High temperature, 41, 680-687, (2003).

[16]R.P. Taleyarkhan, Vapor explosion studies for nuclear and non-nuclear industries, Nuclear engineering and design, 235, 1061-1077, (2005).

[17]A. Bejan, Convection heat transfer, John wiley & sons, (2013).

[18]J.G. Collier, J.R. Thome, Convective boiling and condensation, Clarendon Press, (1994).

[19]J.-P. Franc, J.-M. Michel, Fundamentals of cavitation, Springer Science & Business Media, (2006).

[20]S. Hartland, Surface and interfacial tension: measurement, theory, and applications, CRC Press, (2004).

[21]C. Borgnakke, R. Sonntag, Fundamentals of thermo-dynamics, 7-th edition ,University of Michigan, Willey, (2009).

[22]V.P. Isachenko, V.A. Osipova and A.S. Sukomel, Heat transfer in Russian, Moscow, Energoatomizdot publication, (1981).

[23]A. Bejan, A.D. Kraus, Heat Transfer Handbook', John Wiley & Sons, Inc., Hoboken, New Jersey, (2003).

[24]Y. Jaluria, K. Torrance, Computational heat transfer. Taylor and Francis, New York, (2003).
[25]W. Fritz, In VDI-Wärmeatlas, Düsseldorf Hb2, (1963).
[26]W .Wagner, A. Pruß, The IAPWS formulation 1995 for the thermodynamic properties of ordinary water substance for general and scientific use, Journal of physical and chemical reference data, 31, 387-535, (2002).
[27]O. Rebas, H. Zait, N. Sk, E. Chitour, Prediction of the enthalpy of vaporization according to the temperature far from the critical point by the group contribution method with interactions of pure hydrocarbons, simple mixtures and oil fractions, Journal of Petroleum and Gas Engineering, 7, 132-145, (2011).
[28] A. Jahangiri, Modeling the growth of a vapor film formed in contact between a hot metal sphere and water in pressure vessels. Proceedings of the Institution of Mechanical Engineers, Part E: Journal of Process Mechanical Engineering. 2018. https://doi.org/10.1177/0954408918760894.
[29] A. Jahangiri, M. Biglari, The stability of vapor film immersed in superfluid helium on the surface of the hot ball Proceedings of the Institution of Mechanical Engineers, Part E: Journal of Process Mechanical Engineering, 230(6),433-439,(2016).
[30] A. Jahangiri, M. Biglari, Thermo-physical investigation of the explosive rapid boiling during the contact of a single water drop with liquid methane. Proceedings of the Institution of Mechanical Engineers, Part E: Journal of Process Mechanical Engineering, 229(4), 256-264, (2015).